

# Modelling seagrass competition in the Mediterranean Sea in global warming scenarios

Eva Llabrés<sup>1</sup>, Aina Blanco-Magadán<sup>2</sup>, Marta Sales<sup>2</sup>, and Tomàs Sintès<sup>1</sup>

<sup>1</sup>*Institute for Cross-Disciplinary Physics and Complex Systems, IFISC (CSIC-UIB), Universitat de les Illes Balears, E-07122 Palma de Mallorca, Spain*

<sup>2</sup>*Observatori Sociambiental de Menorca, Institut Menorquí d'Estudis, 07702 Maó, Spain*

May 2, 2022

## Abstract

Temperature anomalies in the coastal water are expected to intensify in the next years due to global climate change. Temperature elevation has been observed to strongly affect the ecosystems of seagrass meadows worldwide, decreasing the shoot density, biomass, and leaf productivity. This effect will be particularly relevant in the Mediterranean Sea in which endemic seagrasses *P. oceanica* and *C. nodosa* show a different response to the thermal stress. The changes in the species competition will alter the growth dynamics, their spatial distribution, and, consequently, the ecosystem functionality.

In this article, we use a mathematical model based on the clonal growth of seagrasses to study the competition between *P. oceanica* and *C. nodosa*. One of our main findings is the identification of a region of coexistence located at the borders between patches of mono-specific species. This region has the shape of a stripe and the model predictions are found to be in agreement with field observations performed in Ses Olles de Son Saura (Balearic Islands, Western Mediterranean Sea). Such comparison allowed us to evaluate the cross-species interaction parameters through the measurement of the width of the coexistence region.

Previous observations show that the mortality of *P. oceanica* alarmingly increases with seawater temperature, while *C. nodosa* has a higher thermal resilience. It is expected that in the following decades *C. nodosa* will become the predominant seagrass in the Mediterranean Sea, replacing the substrate previously occupied by *P. oceanica*. In a positively-moderate scenario of carbon emissions and local disturbances, our model predicts a total invasion of *C. nodosa* by the year 2072, and the functional extinction of *P. oceanica* in the year 2076 in locations with similar environmental conditions to the study site.

## INTRODUCTION

Seagrass meadows are one of the most valuable structural elements in marine coastal areas since they provide ecosystem services in the form of nutrient supply, refuge, and nursery ground to many species of fishes and invertebrates [Costanza et al., 1997]. In addition to support marine

biodiversity, they create architectural structure as benthic producers, contribute to the water quality and sediment stabilization [Orth et al., 2006], and are responsible for globally significant carbon sequestration [Duarte et al., 2005]. Despite their relevance, seagrass ecosystems are under global threat due to anthropogenic factors, being global warming one of the major drivers behind their loss [Waycott et al., 2009]. It is specially alarming the case of areas that exhibit rapid warming rates, such as the Mediterranean Sea. The Mediterranean Sea warms up three times faster than the global ocean, and it has an increased occurrence of extreme temperature events [Vargas-Yáñez et al., 2010]. Future higher temperatures will have consequences in the distribution of seagrass beds, consequently affecting their associated ecosystems [Marbà and Duarte, 2010, Jordà et al., 2012].

*P. oceanica* and *C. nodosa* are the most common and widespread species of seagrasses in the Mediterranean Sea. Their dynamics and associated ecosystem services are conditioned by the different morphological and physiological features of the two plants [Mazzella et al., 1993]. For example, *P. oceanica* forms robust meadows, with thick, long-living rhizomes, that extend both vertically and horizontally. Their leaves are commonly 1m long and generate a significant amount of biomass. This is in contrast with *C. nodosa*, which has much thinner and shorter leaves, and a simpler rhizomatic structure lacking vertical growth. These features make *P. oceanica* a more efficient ecosystem engineer than *C. nodosa*, with enhanced benthic production, a larger associated animal community, and a higher carbon burying capacity [Marbà et al., 1996, Duarte and Chiscano, 1999]. The two plants have also different growth strategies: while *C. nodosa* has regular flowering events every year, sexual reproduction is irregular and uncommon in *P. oceanica* [Pergent-Martini et al., 1994]. As a consequence, *C. nodosa* has higher phenotypical plasticity and a superior capacity for adaption. Also, *C. nodosa* possesses fast colonization patterns, contrarily to the slow rhizome growth rate of *P. oceanica* [Marbà et al., 1996]. These characteristics make *P. oceanica* extremely vulnerable to changes in the environmental conditions, such as an increase in seawater temperature [Marbà and Duarte, 2010]. Previous predictions indicate that *P. oceanica* meadows will become functionally extinct by the middle of this century due to global warming, even in scenarios with mild carbon emissions [Jordà et al., 2012], while *C. nodosa* might even enhance growth in these conditions [Savva et al., 2018]. It is expected that in the following decades *C. nodosa* will become the predominant seagrass in the Mediterranean Sea, replacing substrate previously occupied by *P. oceanica* [Chefaoui et al., 2018].

The study of the growth dynamics and the changes in the space occupation of competing seagrasses in response to an increased temperature is necessary to anticipate to the possible consequences of global warming. Mathematical models for seagrasses provide a theoretical framework to study the most relevant mechanisms that govern the dynamics of these ecosystems, and they can predict possible future scenarios subjected to different environmental conditions. In this work, we have extended previous models based on plant clonal growth [Sintes et al., 2005, Llabrés et al., 2022] to make predictions about the changes in the space distribution of *P. oceanica* and *C. nodosa* in different global warming scenarios, and to study the mechanisms behind the interaction of these two species.

# MATERIALS AND METHODS

## Numerical model

In this article, we study the interactions between the seagrasses *C. nodosa* and *P. oceanica* using the agent-based model proposed in [Llabrés et al., 2022, Sintes et al., 2005]. The model follows a set of growth rules, based on the clonal behavior of the plant, and related to the following empirical parameters: the rhizome elongation rate [ $v$ ], that sets the horizontal spread of the clone; the branching rate [ $\nu_0$ ], that controls the capacity of the clone to form dense networks; the branching angle [ $\phi$ ], that determines the efficiency of the space occupation; the spacer length [ $\delta$ ], that measures the length of the piece of rhizome between consecutive shoots; and the shoot mortality rate [ $\mu$ ] [Bell and Tomlinson, 1980, Marbà and Duarte, 1998]. For more details on the implementation of the model, see Supplementary Material A. The values of the clonal growth parameters are collected with direct experimental observations, and shown in Table 1 for each species.

	Spacer length	Rhizome elongation	Branching rate	Branching angle	Mortality
Symbol	$\delta$	$v$	$\nu_0$	$\phi$	$\mu_0$
Units	cm	cm yr <sup>-1</sup> apex <sup>-1</sup>	branches yr <sup>-1</sup> apex <sup>-1</sup>	degree	yr <sup>-1</sup>
<i>P. oceanica</i> (1)	2.87	6.11	0.05	49	0.03 - 0.07
<i>C. nodosa</i> (2)	3.7	160	2.3	46	0.92

Table 1: *Posidonia oceanica* and *Cymodocea nodosa* clonal growth parameters. Their values are found by direct experimental observation. For *C. nodosa*, we refer to [Terrados et al., 1997, Duarte and Sand-Jensen, 1996, Duarte and Sand-Jensen, 1990], and for *P. oceanica* to [Marbà and Duarte, 1998, Marbà and Walker, 1999]. The values of the *P. oceanica* constant mortality rate ( $\mu_0$ ) are fixed two different values: 1)  $\mu_0 = 0.03yr^{-1}$ , to reproduce stable density meadows, and 2)  $\mu_0 = 0.07yr^{-1}$ , to consider local disturbances that cause the deterioration and death of the meadows [Jordà et al., 2012].

Local interactions among shoots are incorporated into the model via a density-dependent branching rate [Llabrés et al., 2022], i.e.  $\nu(\rho) = \nu_0 + \alpha\hat{\rho}(1 - \hat{\rho})$ , where  $\hat{\rho} = \rho/\rho_{max}$  is the normalized local density, and  $\alpha$  is a coefficient that controls the strength of the interaction. The parabolic shape of  $\nu(\rho)$  penalizes over- and under-populated areas and favors regions around an optimal density  $\rho = \rho_{max}/2$ . To include interactions among two different species (1 & 2), the local density is generalized to  $\hat{\rho}_i = (\rho_i + \gamma_{ij}\rho_j)/\rho_{max,i}$ , where  $\gamma_{ij}$  is the coupling coefficient and  $i \neq j = 1, 2$ . The higher the value of  $\gamma_{12}$  is, the more the seagrass species 1 is affected by the presence of species 2., and vice-versa. The coupling coefficients  $\gamma_{ij}$  cannot be fixed by direct measurements and must be inferred indirectly by comparing the solutions of the model to field observations. The outcomes of the simulations were inspected in [Llabrés et al., 2022], and the following two cases were distinguished:

- **Mixed meadows:** Stable mixed meadows are able to develop when the interaction parameters satisfy the inequalities:  $\gamma_{12} < 1$  and  $\gamma_{21} < 1$ . In this case, the self-interaction is higher than the inter-specific interaction for both species, and the competition is minimized when they mix.
- **Mono-specific meadows:** The condition  $\gamma_{12} > 1$  ( $\gamma_{21} > 1$ ) favours the self-interaction between individuals of species 1 (2) and causes species to separate into mono-specific domains.

In this work, we study the interactions between *P. oceanica* (1) and *C. nodosa* (2). *P. oceanica* has a stronger rhizomatic structure, and much longer and thicker leaves than *C. nodosa* [Mazzella et al., 1993]. Therefore, we will assume that *P. oceanica* grows almost unaffected by the presence *C. nodosa*. In all simulations, we fix  $\gamma_{12} = 0.1$  and explore the response for different values of  $\gamma_{21} > 1$ . This combination of coupling parameters will result in domain separated solutions for *P. oceanica* and *C. nodosa*. The optimal density for both species is selected to  $\rho_{max,1} = 1800$  shoots/ $m^2$ ,  $\rho_{max,2} = 2400$  shoots/ $m^2$ , close to the experimental values measured in the Balearic Sea [Vaquer-Sunyer and Barrientos, 2021]. We also fixed  $\alpha_i = \nu_{0,i}/2$ , such that the order of the effective branching rates  $\nu_i(\rho)$  is consistent with observations.

One of the main goals of this article is the study of the temperature effects in the dynamics of seagrasses in the Mediterranean Sea. Previous results, based on field observations, indicate that natural populations of *P. oceanica* increase their mortality rate linearly with  $\mu \approx 0.028 SST_{max}$ , where  $SST_{max}$  is the yearly maximum of the surface seawater temperature [Marbà and Duarte, 2010]. In the present paper, we will assume that warming also grows linearly with time  $t$ :  $SST_{max} \approx \lambda t$ . The parameter  $\lambda$  is the increase rate in the seawater temperature, and its value can be tuned to model future warming scenarios. *C. nodosa* is not negatively affected by seawater temperatures below 34°C [Savva et al., 2018], and we will consider its mortality rate to be constant.

In our simulations, we have used a system size of  $L \times L$ , with  $L = 20 m$  and periodic boundary conditions. A square grid, representing the quadrant placed in the meadow, is superimposed on top of the continuum space. The grid spacing is set to 20 cm, and it is used to measure the average shoot density and other relevant magnitudes in the simulations. The results have been averaged over 15 independent realizations.

## Experimental design

The field observation was conducted in Ses Olles de Son Saura, located on the north coast of Menorca (Balearic Islands, Western Mediterranean Sea) in October 2021. The site is a sheltered cove with an estimated surface area of 0.3 km<sup>2</sup>. The fieldwork was performed in areas with a maximum depth of 2 m that were covered by the seagrasses *P. oceanica* and *C. nodosa*. The two plants organized in mono-specific meadows occupying different domains of the seafloor. However, we could often identify a narrow and well defined *coexistence region* at the frontier between meadows, which had the appearance of a stripe with a seemingly regular width (Fig. 1). A minimum of five different coexistence regions were analysed in the study site. We measured the width, *C. nodosa* shoot density, and *P. oceanica* leaf length in a couple of randomly selected points at each front. Shoot density was measured by counting the number of shoots in a 20 × 20 cm quadrant. Points with less than seven shoots of *P. oceanica* or *C. nodosa* were not considered. We also randomly selected seven *P. oceanica* leaves per quadrant, measured their length from ground to tip, and performed their average. The width at each of the selected regions of coexistence was measured from the outer-most shoot of *P. oceanica* to the outer-most shoot of *C. nodosa* at each side of the stripe.

We also measured 1420 shoots/ $m^2$  for the average shoot density in *C. nodosa* mono-specific meadows at the location. This data is comparable to the shoot density 1450 shoots/ $m^2$ , collected in June 2021 during the seasonal peak in seagrass biomass and shoot density [Mascaró et al., 2014]. This observation indicates that the measurements in this work will not be significantly different if they would have been collected during the season of *C. nodosa* maximal growth.

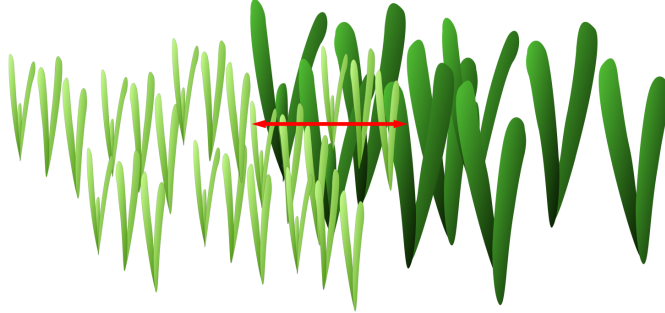


Figure 1: Schematic drawing of the coexistence regions observed in Olles de Son Saura (Balearic Islands, Western Mediterranean Sea). Light green shoots represent seagrass *C. nodosa*, and dark green shoots correspond to *P. oceanica*. The red arrow exemplifies the measurements taken of the coexistence region width.

## RESULTS

### Fronts

We consider a scenario where *P. oceanica* and *C. nodosa* are located in separated domains. We start by fixing the coupling coefficients to  $\gamma_{12} = 0.1$  and  $\gamma_{21} = 6$  (Fig. 2), assuming that the influence of *C. nodosa* over *P. oceanica* is almost negligible, as expected by their anatomy [Mazzella et al., 1993]. The simulation starts at  $t = 0$ , with a 1m wide vertical stripe of homogeneously distributed *P. oceanica* seeds at  $x = -10m$ . When the meadow reaches its stable density at  $t = 46yr$ , we add a similar stripe of *C. nodosa* at  $x = 10m$ . These initial conditions are chosen to generate stable meadows of comparable size for both species, as in Fig. 2 at  $t = 50yr$ . The striped meadows keep growing wider with time until they encounter each other (Fig. 2,  $t = 60yr$ ). Provided the coupling coefficients, the two species do not mix and remain separated in clear domains after the collision. The condition  $\gamma_{21} \gg 1 \gg \gamma_{12}$  ensures that the dominant species is *P. oceanica*, that keeps on winning space over *C. nodosa* (Fig. 2,  $t = 190, 270yr$ ).

In Fig. 2(a), we plot the average density of both species in function of time, and we observe that the *C. nodosa* completely disappears at  $t = 300yr$ . In Fig. 2(b), we plot the density profile along the spatial x-direction for both species at  $t = 190yr$ . We observe that the average shoot density is constant at the interior, but decays towards the outer limits of the meadow. The overlap of density curves for the different species indicates the presence of a region of coexistence at the front. In the snapshots of Fig. 2, this region is represented by the narrow green stripes at the borders between domains.

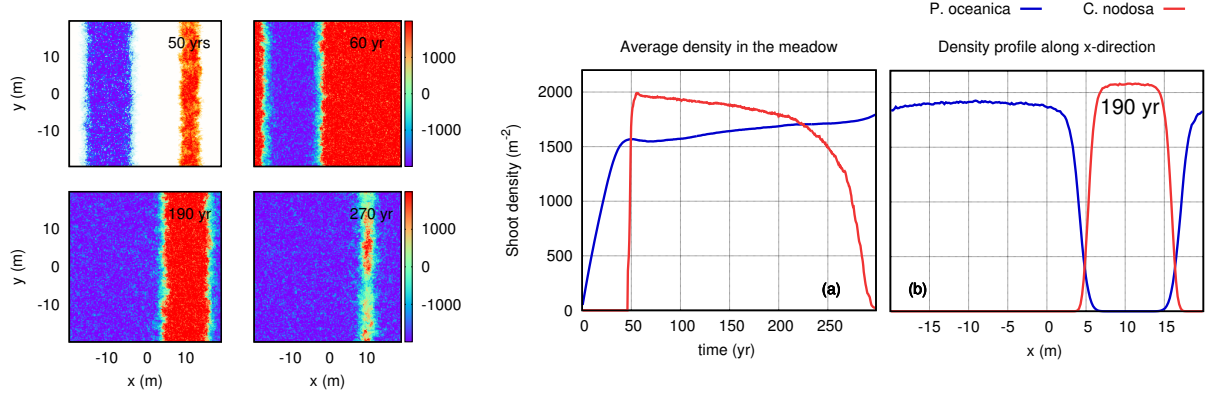


Figure 2: Domain separation of *P. oceanica* and *C. nodosa* with coupling coefficients  $\gamma_{12} = 0.1$  and  $\gamma_{21} = 6$ . Different snapshots are taken at times  $t = 50, 60, 190, 270 \text{ yr}$ , whose color bar shows the difference between  $\rho_{Po} - \rho_{Cn}$ , and it has units of shoots/ $m^2$ . Regions colored in blue (red) are dominated by the presence of *P. oceanica* (*C. nodosa*), and the color green represents regions of coexistence between both species. We also plot the evolution of the average shoot density (a), and the shoot density profile along the x-horizontal direction at  $t = 190 \text{ yr}$  (b).

In Fig. 3, we study the dynamics of the coexistence region at the front between *P. oceanica* and *C. nodosa* for different values of the coupling coefficient  $\gamma_{21} > 1$ . Our main observation is that the width and shoot density at the coexistence region depend on the value of the coupling coefficient  $\gamma_{21}$ . From Fig. 3(a, c), we observe that the shoot densities and the width of the coexistence region remain constant with time. However, the values of these magnitudes vary with  $\gamma_{12}$  (Fig. 3(b, d)). This behavior is related to the spatial shoot density profile, which generally decreases at the outer boundaries of a meadow (Fig. 2(b)). The coupling coefficient  $\gamma_{21}$  dictates the value of the *P. oceanica* shoot density below which coexistence with *C. nodosa* emerges. The higher the values of  $\gamma_{21}$ , the more the density of *C. nodosa* is negatively affected by the presence of *P. oceanica*, and the narrower and less populated is the front (Fig. 3(b,d)). We conclude that *C. nodosa* cannot penetrate into a *P. oceanica* meadow with a high and stable average shoot density. However, since shoot density values decreases at the front, *C. nodosa* can invade a region of the *P. oceanica* meadow.

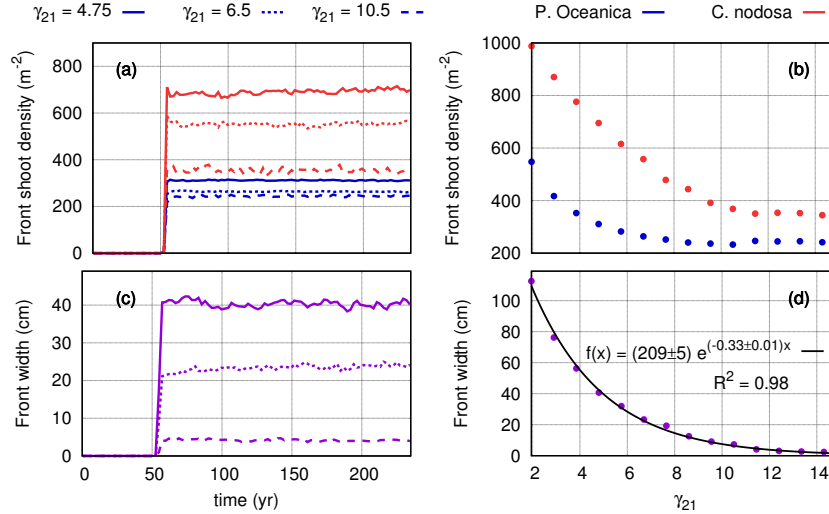


Figure 3: Analysis of the coexistence between *P. oceanica* and *C. nodosa* at the front. (a) Evolution of the shoot density at the coexistence region for selected values of  $\gamma_{21}$ . (b) The saturation shoot densities at the front vs. the coupling coefficient  $\gamma_{21}$ . (c) Evolution of the average width of coexistence region for selected values of  $\gamma_{21}$ . (d) The width of the front vs. the coupling coefficient  $\gamma_{21}$ . The solid back line represents the fit to an exponential decay function. The width is calculated using the formula  $width = r_c N_{coex} / 2 N_y$ , where  $N_{coex}$  is the number of  $20 \times 20 cm$  cells where there is coexistence of species, and  $N_y$  are the number of cells in the  $y$ -axis. As it is done in the experimental methodology, cells with less than seven shoots of any of the species where not considered as part of the coexistence region.

## Experimental observations and comparison to simulations

We have observed stripe-patterned coexistence regions between mono-specific meadows of *P. oceanica* and *C. nodosa* in Ses Olles de Son Saura (Balearic Islands, Western Mediterranean Sea). The measured coexistence regions are found to have an average width of  $21 \pm 2 cm$ , and a *C. nodosa* shoot density of  $613 \pm 70 cm^{-2}$ . Remarkably, the predictions of the numerical model described in the previous sections are in agreement with these findings, where the best fit to the observed data (see Figs. 3(b,d)) suggests a value for the coupling parameter of  $\gamma_{21} \sim 6.5$ .

We also measured an average length of *P. oceanica* leaves at the coexistence region of  $8.15 \pm 0.3 cm$ . This value is considerably lower than the expected one for *P. oceanica* in stable and healthy meadows ( $\sim 1m$ ) [Mazzella et al., 1993]. This observation may indicate that particularly short *P. oceanica* leaves are required for the appearance of coexistence fronts. In addition, we found a negative experimental relationship between the width of the front and the average leaf length of the seagrass *P. oceanica*, that is best fitted by an exponential decay function (Fig. 4). Our simulations also indicate an exponential decrease in the front width with increasing values of the coupling coefficient  $\gamma_{21}$  (Fig. 3(d)). The comparison between both fits suggests an approximately linear dependence between the coupling coefficient  $\gamma_{21}$  and the leaf length of *P. oceanica*. As a consequence, we can identify the leaf length of *P. oceanica* as a possible mediator of interactions between the seagrasses *P. oceanica* and *C. nodosa*.

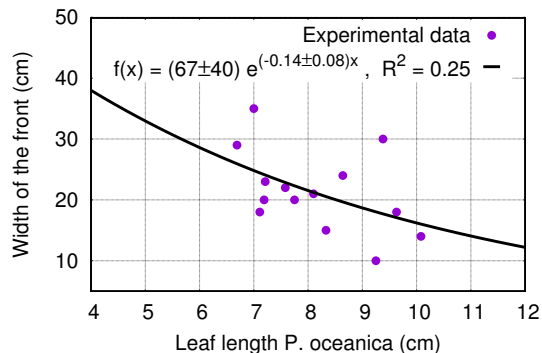


Figure 4: Experimental data at the coexistence fronts in Ses Olles de Son Saura (Balearic Islands, Western Mediterranean Sea). The purple dots represent the shoot density of *C. nodosa* vs. leaf length of *P. oceanica*, and the solid black line corresponds to an exponential fit.

## Temperature

In this section, we study the response of *P. oceanica* to an increase of the sea water temperature via a change in the shoot mortality rate. We start the simulation with a branching and a mortality rates that generate a stable density meadow of *P. oceanica* ( $\nu_0 = 0.02yr^{-1}$  and  $\mu_0 = 0.03yr^{-1}$ ). At time  $t = 0$ , we assume a mortality rate that depends linearly with time in order to include the global warming effects and also possible local disturbances:

$$\mu(t) = \alpha t + \mu_0, \quad (1)$$

where  $\alpha = 0.028 \lambda$ , with  $\lambda$  being the increase rate of the surface water temperature that is assumed linear in time [ $^{\circ}C \cdot yr^{-1}$ ]. The factor 0.028 accounts for the dependence of the mortality of *P. oceanica* with water temperature [ $^{\circ}C^{-1} \cdot yr^{-1}$ ] [Marbà and Duarte, 2010]. At  $t = 0$ , we set the mortality rate to  $\mu_0 = 0.07yr^{-1}$ . This value takes into account the local disturbances that deteriorate the meadow. Afterwards, the mortality increases at a rate that depends on  $\lambda$ . We perform the simulation in three different sea warming scenarios:  $\lambda = 0.6, 2.76, 13.8^{\circ}C/100 yr$ . The rate  $2.76^{\circ}C/100 yr$  was predicted by [Jordà et al., 2012] using a positively-moderate scenario of carbon emissions (A1B) from the Special Report on Emissions Scenario from the IPCC [Nakicenovic and Swart, 2000]. The rates 0.6 and  $13.8^{\circ}C/100 yr$  have been chosen to evaluate the sensitivity of the model to a variation of the sea water temperature increase rate. In Fig. 5(a), we observe that meadows reduce to a 10% of its initial density at different times ( $t = 31, 56, 86 yr$ ) depending of the mortality rate. In Fig 5(b), we plot in a semi-logarithmic scale the change in the number of shoots ( $N$ ) with time ( $t$ ). We observe that the dependence is quadratic implying an exponential decay of the form:  $N(t) = \exp(at^2 + bt + c)$ . The best fit for the coefficients  $a, b, c$  are summarized in Table 2 for the different values  $\lambda$ . From the homogeneous solutions to the model equations (See SM Sec. B) we could derive a relationship between the  $a, b, c$  constants and the model parameters:  $a = -0.028 \lambda/2$ ,  $b = (\nu - \mu_0)$  and  $c = \log(N_0)$ . These relations are deduced neglecting shoot local interactions. However, we observe in Table 2 that they still yield a good approximation, at least for our parameter choice. It is also interesting to point out that the dominant quadratic term is accompanied by the factor  $\lambda$ , which indicates that the regression of *P. oceanica* is led by an increase of the sea water



temperature.

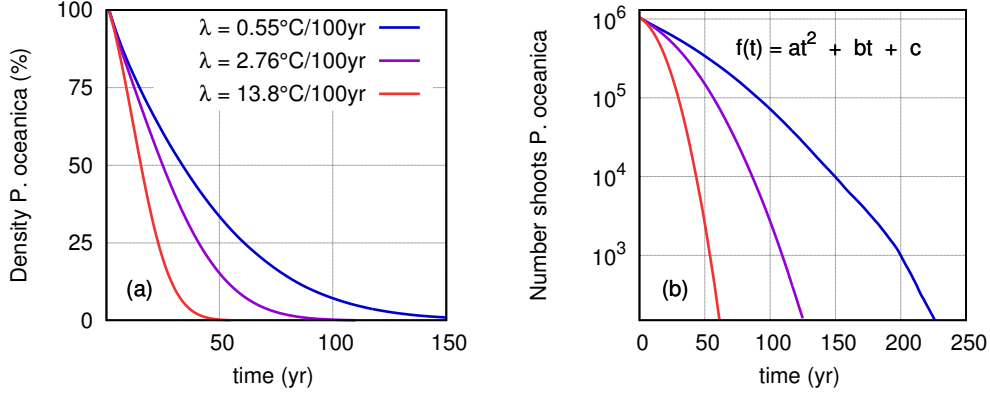


Figure 5: Population decay in *P. oceanica* meadows subjected to different global warming scenarios. The mortality rate of the seagrass increases linearly with time:  $\mu(t) = \alpha t + \mu_0$ . The initial mortality rate is fixed to  $\mu_0 = 0.07 \text{ yr}^{-1}$ , the branching rate is  $\nu_0 = 0.05 \text{ yr}^{-1}$ , and  $\alpha = 0.028\lambda$ , where  $\lambda$  is the sea temperature increase rate. The two subfigures represent: (a) the percentage of shoot density loss for the selected, and the (b) evolution of the number of shoots in logarithmic scale. We observe a quadratic dependence on time, best fitted by the function  $f(t) = at^2 + bt + c$ , with the values of  $a, b, c$  displayed in Table 2.

$\lambda$ $^\circ\text{C}/100\text{yr}$	$a$ $\text{yr}^{-2}$	$b$ $\text{yr}^{-1}$	$c$ adim.	$-\alpha/2$ $\text{yr}^{-2}$	$\nu - \mu_0$ $\text{yr}^{-1}$	$\log(N_0)$ adim.
0.55	$(-1.00 \pm 0.01) \cdot 10^{-4}$	$-0.016 \pm 0.003$	$13.75 \pm 0.01$	$-0.8 \cdot 10^{-4}$	-0.02	13.85
2.76	$(-4.28 \pm 0.05) \cdot 10^{-4}$	$-0.0172 \pm 0.0007$	$13.790 \pm 0.002$	$-3.9 \cdot 10^{-4}$	id.	id.
13.8	$(-2.06 \pm 0.01) \cdot 10^{-3}$	$-0.0210 \pm 0.0002$	$13.816 \pm 0.002$	$-1.9 \cdot 10^{-3}$	id.	id.

Table 2: Parameters from the fit exponential  $f(t) = at^2 + bt + c$  in Fig. 2(b). The comparison between  $a, b, c$  and the model parameters in three last columns shows an agreement between the simulation results and the analytical solution of the model (SM Sec. B).

We consider now the competition effects of *C. nodosa* and *P. oceanica* in the Mediterranean Sea warming scenario predicted by [Jordà et al., 2012], i.e.  $\lambda = 2.76^\circ\text{C}/100\text{yr}$ . In Fig. 6, we start the simulations with the same initial conditions as in Fig. 2. We assume that before year 2020, the seagrasses were not affected by the temperature, and neither by local disturbances. At year 2020, we assume that the mortality rate of *P. oceanica* follows equation (1). *C. nodosa* is thermally resilient [Savva et al., 2018], and its mortality rate will be kept constant. In Fig. 6, we observe that in this situation *P. oceanica* meadows do not displace *C. nodosa* as it happened for constant temperature case. The average total density of *P. oceanica* decreases, and the shoots of *C. nodosa* keep on colonizing the *P. oceanica* meadow. Since the densities in the area of coexistence are lower than in the mono-specific regions, the progressive invasion of the *C. nodosa* causes an initial decrease of its total average shoot density (Fig. 6(a), red curve). The location of the minimum in the density of *C. nodosa* corresponds to the time where the whole meadow of *P. oceanica* has been colonized. In Fig. 6(b), we observe that the time of total invasion is delayed as we increase the coefficient  $\gamma_{21}$ . This behavior is related to Fig. 3(a,b), where the threshold densities for the coexistence of *C. nodosa* and *P. oceanica* are lower for

higher values  $\gamma_{21}$ . Hereafter, *P. oceanica* keeps regressing due to the increase of temperature until its disappearance, leading to the formation of *C. nodosa* mono-specific meadows.

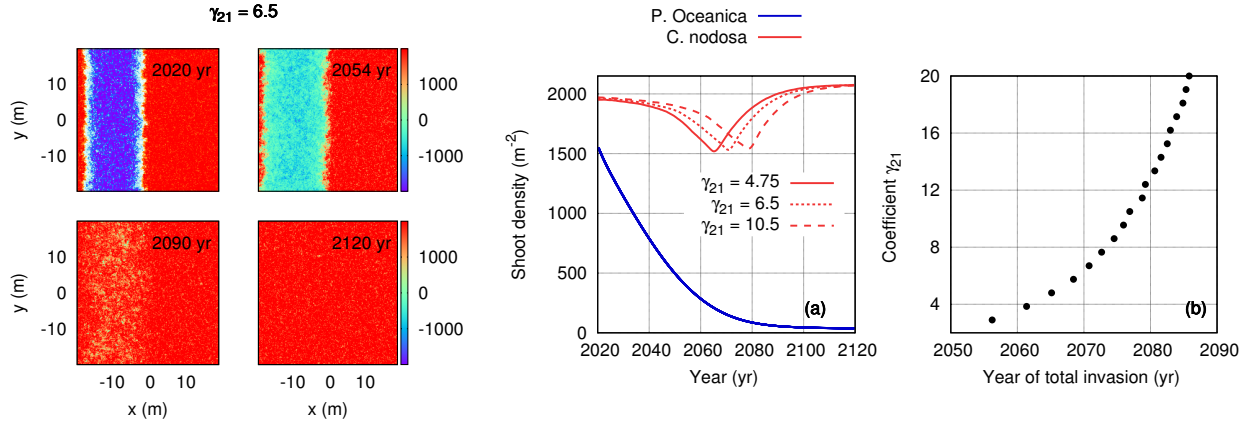


Figure 6: Domain separation of *P. oceanica* and *C. nodosa* in a global warming scenario starting at year 2020. Different snapshots are taken between 2020 and 2120, whose color bar shows the difference between  $\rho_{Cp} - \rho_{Cn}$ , and it has units of shoots/m<sup>2</sup>. (a) The averaged shoot density of both seagrasses is shown for some selected  $\gamma_{21}$ . b) Coupling coefficient  $\gamma_{21}$  vs. the year of total occupation, which corresponds to the lower peak of the red curve in graphic (a).

## Discussion

In this work, we use the mathematical models for seagrasses proposed in [Llabrés et al., 2022, Sintes et al., 2005] to study interactions between *P. oceanica* and *C. nodosa*. One of our main findings is the identification of a region of coexistence at the borders between mono-specific domains. This region has the shape of a stripe, and is found to be in agreement with field observations performed in Ses Olles de Son Saura (Balearic Islands, Western Mediterranean Sea). Comparing the average width of the coexistence region in the study site to the simulation outcomes, we are able to fix the coupling coefficient to  $\gamma_{21} \sim 6.5$ . We also found empirical evidence that unusually short leaves of *P. oceanica*, averaged 8.15cm in the study site, may be necessary for the coexistence with *C. nodosa*. This is related to the scarce light available for *C. nodosa* in the presence of *P. oceanica* with a longer average height. The comparison between field data (Fig. 4) and simulations (Fig. 3(d)) hint a linear relation between the coupling coefficient  $\gamma_{21}$  and the leaf length of *P. oceanica*, which reveals that interactions are possibly mediated by the *P. oceanica* leaf length. Also, short *P. oceanica* leaves are usually an indicator of deterioration in the seagrass, due to nutrient enrichment, urban effluents or fish farms [Short et al., 1995, Leoni et al., 2006, Delgado et al., 1999, Ruiz et al., 2001, Balestri et al., 2004]. This observation implies that multi-specific meadows of both species will only occur when *P. oceanica* suffers from degradation.

We have also used the numerical models to study the effects of global warming over seagrass populations. Our simulations indicate that for seagrass species whose mortality rate increases

linearly with time, i.e.  $\mu(t) = \alpha t + \mu_0$ , the number of shoots decays as:

$$N(t) = N_0 \exp \left[ -\frac{\alpha}{2} t^2 + (\nu_0 - \mu_0) t \right], \quad (2)$$

where  $\nu_0$  is the branching rate, and  $N_0$  the initial number of shoots. This behavior is consistent with the solution of the differential equations describing the population dynamics neglecting local interactions (SM Sec. B), and also expected from the early exponential growth in young patches [Sintes et al., 2005]. Combining field observations of *P. oceanica* shoot mortality rates [Marbà and Duarte, 2010], and the (positively-moderate) predictions for the sea temperature in [Jordà et al., 2012], our model forecasts that stable *P. oceanica* meadows will become functionally extinct (90% density reduction) in 56 years (year 2076). Our results differ from the work in [Jordà et al., 2012], where they project the functional extinction of *P. oceanica* in approximately 39 years. Their estimations are performed using analogous environmental conditions, but considering a population decay of  $N(t) = N_0 \exp [-\alpha t^2 + (\nu - \mu_0)t]$ , disagreeing with (2) by a factor of two in the quadratic term. In this article, we also discuss the implications of sea warming in the distribution of *P. oceanica* and *C. nodosa* seabeds. *C. nodosa* has a higher thermal resilience, and it is expected to replace *P. oceanica* as this deteriorates. In locations with similar environmental conditions than the study site ( $\gamma_{21} \sim 6.5$ ), our mathematical model predicts a total invasion of *P. oceanica* meadows by year 2072 (Fig. 6).

The parameter  $\alpha$  in formula (2) is linearly dependent on the yearly maximum temperature of the sea-water surface ( $SST_{max}$ ). Therefore, our model indicates that global warming and the increase in the number and severity of heatwaves are leading effects causing the alarming loss of *P. oceanica*. The possible extinction of *P. oceanica* and other seagrass species will cause dramatic losses in the biodiversity of coastal ecosystems, have high impacts on their dependent human communities, and reduce the total global capacity of carbon sequestration [Waycott et al., 2009, Duarte et al., 2013]. These concerns are reflected in the Sixth Assessment Report of the Intergovernmental Panel on Climate Change (IPCC) [Shukla et al., 2022], where seagrasses are pointed out as one of the main vulnerable ecosystems requiring special preservation. The report emphasizes that limiting warming to 1.5°C from pre-industrial levels requires gas emissions to peak before 2025 at the latest, and be reduced by 43% by 2030. Beyond this temperature, irreversible losses will occur in terrestrial and marine ecosystems [IPCC, 2014]. For *P. oceanica*, which has very slow rhizome growing rates (1-6 cm/yr) [Marbà et al., 1996], strict conservation measures will be necessary for a complete recovery of the meadows, even after globally achieving net-zero carbon dioxide emissions.

## ACKNOWLEDGMENTS

E.LL. and T.S. acknowledge the Research Grants: PRD2018/18-2 funded by LIET from the D. Gral. d’Innovació i Recerca (CAIB), RTI2018-095441-B-C22 funded by European Regional Development Fund - "A way of making Europe", and MDM-2017-0711 funded by MCIN/AEI/10.13039/501100011033.

## References

- [Balestri et al., 2004] Balestri, E., Benedetti-Cecchi, L., and Lardicci, C. (2004). Variability in patterns of growth and morphology of *posidonia oceanica* exposed to urban and industrial wastes: contrasts with two reference locations. *Journal of Experimental Marine Biology and Ecology*, 308(1):1–21.
- [Bell and Tomlinson, 1980] Bell, A. D. and Tomlinson, P. B. (1980). Adaptive architecture in rhizomatous plants. *Botanical Journal of the Linnean Society*, 80(2):125–160.
- [Chefaoui et al., 2018] Chefaoui, R. M., Duarte, C. M., and Serrão, E. A. (2018). Dramatic loss of seagrass habitat under projected climate change in the mediterranean sea. *Global Change Biology*, 24(10):4919–4928.
- [Costanza et al., 1997] Costanza, R., d’Arge, R., de Groot, R., Farber, S., Grasso, M., Hannon, B., Limburg, K., Naeem, S., O’Neill, R. V., Paruelo, J., Raskin, R. G., Sutton, P., and van den Belt, M. (1997). The value of the world’s ecosystem services and natural capital. *Nature*, 387(6630):253–260.
- [Delgado et al., 1999] Delgado, O., Ruiz, J., Pérez, M., Romero, J., and Ballesteros, E. (1999). Effects of fish farming on seagrass (*posidonia oceanica*) in a mediterranean bay: seagrass decline after organic loading cessation. *Oceanologica Acta*, 22(1):109–117.
- [Duarte, 1989] Duarte, C. (1989). Temporal biomass variability and production/biomass relationships of seagrass communities. *Marine Ecology Progress Series*, 51:269–276.
- [Duarte and Chiscano, 1999] Duarte, C. M. and Chiscano, C. L. (1999). Seagrass biomass and production: a reassessment. *Aquatic Botany*, 65(1):159–174.
- [Duarte et al., 2013] Duarte, C. M., Kennedy, H., Marbà, N., and Hendriks, I. (2013). Assessing the capacity of seagrass meadows for carbon burial: Current limitations and future strategies. *Ocean and Coastal Management*, 83:32–38.
- [Duarte et al., 2005] Duarte, C. M., Middelburg, J. J., and Caraco, N. (2005). Major role of marine vegetation on the oceanic carbon cycle. *Biogeosciences*, 2(1):1–8.
- [Duarte and Sand-Jensen, 1990] Duarte, C. M. and Sand-Jensen, K. (1990). Seagrass colonization: biomass development and shoot demography in *cymodocea nodosa* patches. *Marine Ecology Progress Series*, 67(1):97–103.
- [Duarte and Sand-Jensen, 1996] Duarte, C. M. and Sand-Jensen, K. (1996). Nutrient constraints on establishment from seed and on vegetative expansion of the mediterranean seagrass *cymodocea nodosa*. *Aquatic Botany*, 54(4):279–286.
- [IPCC, 2014] IPCC, C. W. T. (2014). *IPCC, 2014: Climate Change 2014: Synthesis Report. Contribution of Working Groups I, II and III to the Fifth Assessment Report of the Intergovernmental Panel on Climate Change. I.* Number ISBN 978-92-9169-143-2. Cambridge University Press, IPCC, Geneva, Switzerland.
- [Jordà et al., 2012] Jordà, G., Marbà, N., and Duarte, C. M. (2012). Mediterranean seagrass vulnerable to regional climate warming. *Nature Climate Change*, 2(11):821–824.
- [Leoni et al., 2006] Leoni, V., Pasqualini, V., Pergent-Martini, C., Vela, A., and Pergent, G. (2006). Morphological responses of *posidonia oceanica* to experimental nutrient enrichment of the canopy water. *Journal of Experimental Marine Biology and Ecology*, 339(1):1–14.

- [Llabrés et al., 2022] Llabrés, E., Mayol, E., Marbà, N., and Sintes, T. (2022). A mathematical model for inter-specific seagrass interactions: reproducing field observations for *c. nodosa* and *c. prolifera*.
- [Marbà et al., 1996] Marbà, N., Cebrian, J., Enríquez, S., and Duarte, C. (1996). Growth patterns of western mediterranean seagrasses: species-specific responses to seasonal forcing. *Marine Ecology Progress Series*, 133.
- [Marbà and Duarte, 1998] Marbà, N. and Duarte, C. (1998). Rhizome elongation and seagrass clonal growth. *Marine Ecology Progress Series*, 174:269–280.
- [Marbà and Duarte, 1998] Marbà, N. and Duarte, C. M. (1998). Rhizome elongation and seagrass clonal growth. *Marine Ecology Progress Series*, 174:269–280.
- [Marbà and Duarte, 2010] Marbà, N. and Duarte, C. M. (2010). Mediterranean warming triggers seagrass (*posidonia oceanica*) shoot mortality. *Global Change Biology*, 16(8):2366–2375.
- [Marbà et al., 1996] Marbà, N., Duarte, C. M., Cebrián, J., Gallegos, M. E., Olesen, B., and Sand-Jensen, K. (1996). Growth and population dynamics of *posidonia oceanica* on the spanish mediterranean coast: elucidating seagrass decline. *Marine Ecology Progress Series*, 137(1/3):203–213.
- [Marbà and Walker, 1999] Marbà, N. and Walker, D. I. (1999). Growth, flowering, and population dynamics of temperate western australian seagrasses. *Marine Ecology Progress Series*, 184:105–118.
- [Mascaró et al., 2014] Mascaró, O., Romero, J., and Pérez, M. (2014). Seasonal uncoupling of demographic processes in a marine clonal plant. *Estuarine Coastal and Shelf Science*, 142:23–31.
- [Mazzella et al., 1993] Mazzella, L., Scipione, M., Gambi, M. C., Buia, M., Lorenti, M., Zupo, V., and Cancemi, G. (1993). The mediterranean seagrass *posidonia oceanica* and *cymodocea nodosa*.
- [Nakicenovic and Swart, 2000] Nakicenovic, N. and Swart, R. (2000). *Emissions scenarios - special report of the Intergovernmental Panel on Climate Change*. Number ISBN 0 521 80493 0. Cambridge University Press.
- [Orth et al., 2006] Orth, R., Carruthers, T., Dennison, W., Duarte, C., Fourqurean, J., Heck, K., Hughes, A., Kendrick, G., Kenworthy, W., Olyarnik, S., Short, F., Waycott, M., and Williams, S. (2006). A global crisis for seagrass ecosystems. *BioScience*, 56(12):987–996.
- [Pergent-Martini et al., 1994] Pergent-Martini, C., Rico-Raimondino, V., and Pergent, G. (1994). Primary production of *posidonia oceanica* in the mediterranean basin. *Marine Biology*, 120:9–15.
- [Ruiz et al., 2001] Ruiz, J. M., Pérez, M., and Romero, J. (2001). Effects of fish farm loadings on seagrass (*posidonia oceanica*) distribution, growth and photosynthesis. *Marine Pollution Bulletin*, 42(9):749–760.
- [Savva et al., 2018] Savva, I., Bennett, S., Roca, G., Jordà, G., and Marbà, N. (2018). Thermal tolerance of mediterranean marine macrophytes: Vulnerability to global warming. *Ecology and Evolution*, 8(23):12032–12043.
- [Short et al., 1995] Short, F., Burdick, D., and Kaldy, J. (1995). Mesocosm experiments quantify the effects of eutrophication on eelgrass, *zostera marina*. *Limnology and Oceanography*.

- [Shukla et al., 2022] Shukla, P. R., Skea, J., Slade, R., Al Khourdajie, A., van Diemen, R., McCollum, D., Pathak, M., Some, S., Vyas, P., Fradera, R., Belkacemi, M., Hasija, A., Lisboa, G., Luz, S., and Malley, J. e. (2022). *IPCC, 2022: Climate Change 2022: Mitigation of Climate Change. Contribution of Working Group III to the Sixth Assessment Report of the Intergovernmental Panel on Climate Change*. Cambridge University Press.
- [Sintes et al., 2005] Sintes, T., Marbà, N., Duarte, C. M., and Kendrick, G. A. (2005). Nonlinear processes in seagrass colonisation explained by simple clonal growth rules. *Oikos*, 108(1):165–175.
- [Terrados et al., 1997] Terrados, J., Duarte, C., and Kenworthy, W. (1997). Experimental evidence for apical dominance in the seagrass *Cymodocea nodosa*. *Marine Ecology Progress Series*, 148:263–268.
- [Vaquer-Sunyer and Barrientos, 2021] Vaquer-Sunyer, R. and Barrientos, N. (2021). *Informe Mar Balear*.
- [Vargas-Yáñez et al., 2010] Vargas-Yáñez, M., Moya, F., Garcia-Martinez, M., Tel, E., Zunino, P., Plaza, F., Salat, J., Pascual, J., Lopez-Jurado, J., and Serra, M. (2010). Climate change in the western mediterranean sea 1900-2008. *Journal of Marine Systems - J MARINE SYST*, 82:171–176.
- [Waycott et al., 2009] Waycott, M., Duarte, C., Carruthers, T., Orth, R., Dennison, W., Olyarnik, S., Calladine, A., Fourqurean, J., Heck, K., Hughes, A., Kendrick, G., Kenworthy, W., Short, F., and Williams, S. (2009). Accelerating loss of seagrasses across the globe threatens coastal ecosystems. *PNAS; Proceedings of the National Academy of Sciences*, 106(30):12377–12381.

## A Implementation of clonal growth rules

Local interactions among shoots are considered using a density dependent branching rate of the form:

$$\nu(\rho) = \nu_0 + \alpha \hat{\rho} (1 - \hat{\rho}), \quad (3)$$

where  $\nu_0$  is the intrinsic branching rate that depends on external factors such as temperature or irradiance [Duarte, 1989],  $\hat{\rho} = \rho/\rho_{max}$  is the normalized local density, and  $\alpha$  is a coefficient that controls the strength of the interaction. Given the parabolic shape of the interaction, the growth of over- and under-populated areas is penalized, whereas regions around an optimal density  $\rho = \rho_{max}/2$  is favoured. Equation (3) can be easily extended to consider the interaction among  $N$  species as follows. We define a normalized local density for the species  $i = 1, \dots, N$  as:

$$\hat{\rho}_i = \frac{1}{\rho_{max,i}} \left( \rho_i + \sum_{j \neq i} \gamma_{ij} \rho_j \right), \quad (4)$$

where  $\rho_{max,i}$  is the saturation density for the  $i$ -species.  $\gamma_{ij}$  is the coupling coefficient between species  $i$  and  $j$ . The normalized density  $\hat{\rho}_i$  is used in Equation (3) to evaluate the branching rate for the  $i$ -species,  $\nu_i(\rho_i)$ . The simulation starts placing a random distribution of seeds (a shoot carrying an apical meristem) of the competing species and assigning to it a unitary vector

$\hat{u}$ , randomly oriented, setting the direction of growth of the rhizome. At each iteration, the following steps are repeated:

1. Since species have different characteristic growing times:  $\tau_i = \delta_i/v_i$ , at each iteration, one of the species is selected with probability  $p_i = \tau_i / \left( \sum_i \tau_i \right)$ .
2. The rhizome that originates in the  $n^{th}$ -apex of the  $i$ -species, randomly selected, is proposed to extend over a distance  $\delta_i \hat{u}_i^{(n)}$ .
3. The apex will be relocated to its new position and a new shoot will develop only if the normalized local density in the corresponding cell, given by the Equation (4), fullfils:  $\hat{\rho}_i < 1$ .
4. Time is increased by  $\Delta t = \delta_i / (v_i N_a^T(t))$ , where  $N_a^T(t)$  is the total number of apices from all species at time  $t$
5. A new branch with a growing apex will develop according to the branching rate  $\nu_i(\rho_i) = \nu_{0i} + \alpha_i \hat{\rho}_i (1 - \hat{\rho}_i)$  with probability:  $p_{\nu,i}(t) = \nu_i(\rho_i) \Delta t N_{a,i}(t)$ , with  $N_{a,i}(t)$  the number apices of the  $i$ -species.
6. During this time step, a number of shoots of the  $i$ -species are removed with probability  $p_{\mu,i}(t) = \mu_i \Delta t / N_{s,i}(t)$ , with  $N_{s,i}(t)$  the number shoots of the  $i$ -species.

## B Differential equations to model regressive meadows

Seagrass shoots are modeled by the following differential equation describing the evolution of a decaying population:

$$\frac{dN(t)}{dt} = -\omega N(t), \quad (5)$$

where  $N(t)$  is the number of shoots at time  $t$ , and  $\omega$  is the net mortality rate. For time-dependent  $\omega = \omega(t)$ , the generic solution to equation (5) is:

$$N(t) = N_0 e^{-\int_t dt' \omega(t')}. \quad (6)$$

For constant  $\omega$ , equation (6) boils down to the exponential  $N(t) = N_0 e^{-\omega t}$ . The net mortality rate of a meadow is often represented as the difference  $\omega = \mu - \nu_0$ , where  $\mu$  is shoot mortality rate, and  $\nu_0$  is the recruitment rate or branching rate. Performing the integral at the exponent (6), for a time mortality rate  $\mu(t) = \alpha t + \mu_0$ , and neglecting local interactions ( $\nu_0$  is constant):

$$N(t) = N_0 \exp \left[ -\frac{\alpha}{2} t^2 + (\nu_0 - \mu_0) t \right]. \quad (7)$$

The previous expression shows a quadratic exponential decay in seagrass populations when the mortality rate is linearly increasing in time.